Circular Distribution of Corona Current of Multiple-Conductor Transmission Line (V)

Saburo MUTO, Toshio SHIBATA and Masaharu UDAKA

Department of Electrical Engineering

(Received September 11, 1968)

In this 5th paper the authors mainly deal with the comparison of the circular distribution of d.c. corona current of multiple-conductor transmission line in CO_2, SF_6, c-C_4F_8 and C_2F_6 by means of the oblique coordinate. The corona starting voltages in perfluorocarbons were measured. The results of the gaschromatographic analysis gave that c-C_4F_8 was probably decomposed by corona discharge.

1. Introduction

This paper follows the investigations of the corona current distribution around the double-conductor which have been already reported for the past four times.[(1)~(4)]

The 1st and 2nd reports dealt with the various characteristics of the corona current around the double-conductor in air at atomospheric pressure and in the 3rd report the characteristics in air pressure lower than atmosphere have been described. In the 4th the d.c. corona current distribution around the double-conductor in N_2, CO_2 and SF_6 (10 Torr to 7kg/cm^2 abs.) have been investigated in detail.

In the 5th the authors make a comparative study of the recent experimental results of the corona current distribution in organic fluoride gases like octafluorocyclobutane (c-C_4F_8) and hexafluoroethane (C_2F_6), and of the previous results.

2. General Characteristics of Perfluorocarbons and SF_6

The general characteristics of the organic fluoride gases used are described as follows.

c-C_4F_8 is comparatively new perfluorocarbon with which Du Pont in U. S. A. deals as commercial products since the 1950's and the molecular structure[(5)] with three kinds of the isomers is shown in **Fig. 1**. The general physical characteristics are shown in **Table 1**[(6)] with C_2F_6, SF_6 and N_2 are also listed up for comparison.

The perfluorocarbons, so-called Freon, have been developed for cooling medium and

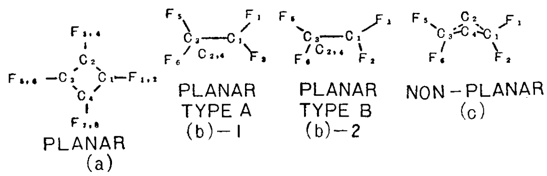

Fig. 1 Molecular Structure of c-C_4F_8

Table. 1 Physical properties of Gases used

		c-C_4F_8	C_2F_6	SF_6	N_2
Molecular Weight		200.04	138.02	146.07	28
Boiling Point	℃	−5.85	−78.2	(Sublimitation) −63.8	−196
Freezing Point	℃	−41.4	−100.6	−50.8(2.3 ata)	
Critical Temp.	℃	115.3	24.3	45.6	−119
Critical Press.	atm	27.5	33.7	38.35kg/cm^2	
Specific Heat	Cal/g·℃	0.190(1atm)	0,082(0atm)	0.144	0.244
Toxicity		Non	Non	Non	

generally their boiling points are comparatively high. When $c\text{-}C_4F_8$ is used as insulating medium, its high boiling point is worth considering. C_2F_6 is not so new perfluorocarbon, but recently it has been advocated to mix C_2F_6 with $c\text{-}C_4F_8$ to compensate for the high boiling point, when $c\text{-}C_4F_8$ is used for electrical insulation. From the viewpoint of the thermal stability, the perfluorocarbons are superior to SF_6. On the other hand, perfluorocarbons are easily decomposed[7] by the injection of high electrical energy like arc.

$c\text{-}C_4F_8$ in ordinary state is not toxic[8] for human body and the thermal stability[9] is very excellent, while are not well known the kind and the amounts of the products which are decomposed by the injection of electical energy like corona discharge.

Pure C_2F_6 is known to be of nontoxity.[6]

3. Measuring Apparatus and Method

In the previous report[4] are shown the details of the measuring equipment of the corona current distribution and, therefore, it would be sufficient only to mention its dimensions here in this report, as shown in **Fig. 2**.

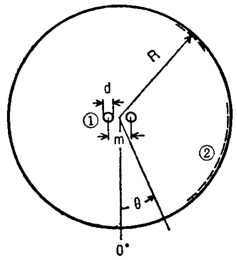

1 Inner Electrodes are of Two Piano Wires.
2 Outer Electrodes are of 36 Strips of Aluminum Foil.
$d=0.3$mm,
$m=3.0$mm,
$R=49.5$mm.

Fig. 2 Cross Section of Electrodes

The measuring method is also the same as that of the previous report.[4] The terminal voltage across the standard resistance means the magunitude of the corona current and its voltage recorded by the automatic balancing potentiometer gives the distribution of the corona current.

X-Y Recorder was used for measuring the corona starting voltage. The total corona current I_t and the applied voltage V were recorded on the Y- and X-axes, respectively. The corona starting voltage is defined as the one corresponding to the abruptly increase point of I_t.

4. Characteristics of Corona Starting in various gases; air, SF_6, $c\text{-}C_4F_8$ and C_2F_6

Fig. 3 shows the corona starting voltages in air, SF_6, $c\text{-}C_4F_8$ and C_2F_6. The maximum voltage-gradient of the corona starting at the surface of the double-conductor, E_{max}, based on the calculation in the previous report[4] is

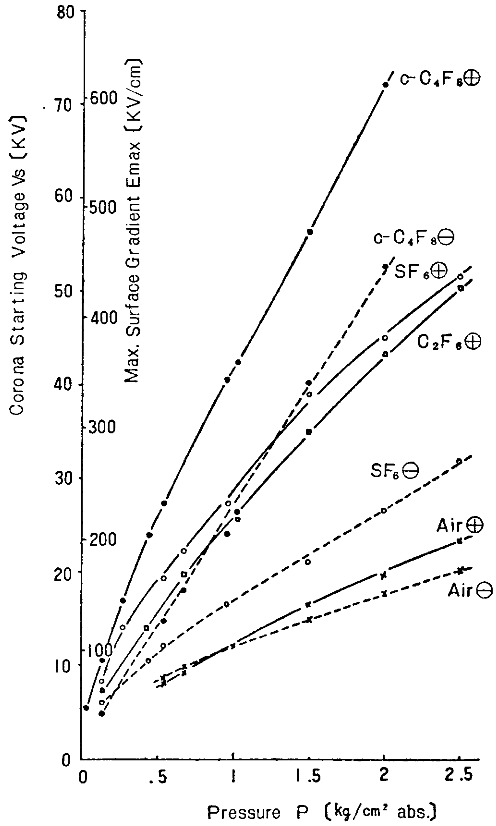

⊕ and ⊖ mean the potentials of the double-conductor to be positive and negative, respectivly.

Fig. 3 Corona Starting Voltage of Double Condctors, $m/d=10$.

also indicated on the ordinate axis. E_{max}, at the applied voltage of V(kV), is given as follows;

$$E_{max}=8.49\times V(\text{kV/cm}) \quad \cdots\cdots(1)$$

In **Fig. 3** the corona starting voltage V_s of CO_2 is omitted because of the complexity of the figure, but V_s of $CO_2\oplus$ is ca. 1kV lower than that of $SF_6\ominus$ and V_s of $CO_2\ominus$ is nearly equal to that of air[4].

The corona starting voltage of $c\text{-}C_4F_8\oplus$ is higher than those of the other gases in overall pressure. In less than 1 atm, however, V_s of c-C_4F_8⊖ is ordinary lower than that of SF_6⊕.

The difference between positive and negative corona starting voltages in c-C_4F_8 is nearly constant, ca. 20kV, in more than 1 atm. On the other hand, the difference between positive and negative V_s's in SF_6 tends to increase as increment of pressure. The corona starting voltage of C_2F_6 is a little lower than that of SF_6, so that from the point of the electrical insulation C_2F_6 is not so attractive as c-C_4F_8. As shown in the previous chapter, however, it has been advocated to use the mixture of C_2F_6 and c-C_4F_8.

Therefore the authors hereafter intend to investigate the corona characteristics in the mixture of C_2F_6 and c-C_4F_8.

As C_2F_6⊖ is now under investigation, the details will be reported in next paper. But the corona starting voltages of C_2F_6⊖ is a little lower than that of SF_6⊖.

5. Comparison of Circular Distribution of Corona Current in various gases

5-1 Circular Distribution of Corona Current of c-C_4F_8⊕

Fig. 4 shows the corona current distribution of c-C_4F_8 under the condition of $I_t=300\mu A$ and 760 Torr.

Now the authors adopt the directivity factor κ in order to analyse the corona current

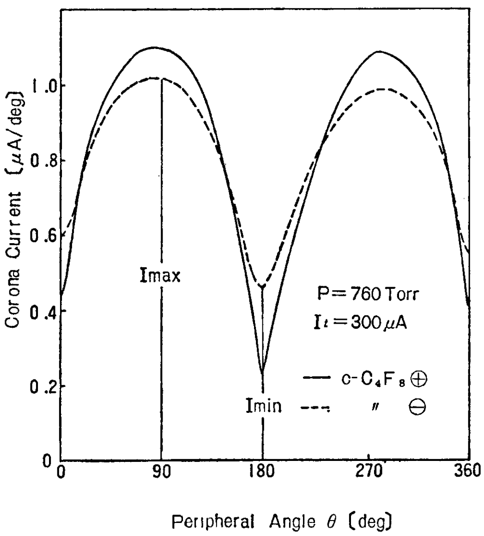

Fig. 4 An Examle of Corona Current Distribution around Double-Condctor in c-C_4F_8

distribution quantitatively as shown in the previous report[4]; namely

$$\kappa=\frac{I_{max}}{I_{min}} \qquad (2)$$

where I_{max} and I_{min} stand for maximum and minimum values of corona current distribution, respectively, as shown in **Fig. 4.**

Consequently the large κ means that the corona current distribution is in a sharp form and $\kappa=1$ means the uniform distribution of the corona current.

5-2 Comparison of Directivities in various gases

Fig. 5 through **Fig. 8** show the κ-I_t-p characteristics of SF_6, CO_2, c-C_4F_8 and C_2F_6, respectively, by means of the oblique coordinates, where p stands for gas pressure. κ and I_t axes are graduated in logarithms.

κ-I_t characteristics of SF_6 and CO_2, which correspond to the projections to the κ-I_t planes of the figures, show good linearities and the experimental formula[4] is given as follows;

$$\kappa I_t^B=A, \qquad (3)$$

where A and B are constants determined by the kinds of gases, pressure, polarity and total corona current.

The κ-I_t characteristics of c-C_4F_8 and C_2F_6, however, do not show always linearities. It is thought that the ion cluster, whose mobilities are fairly small because of the large masses of c-C_4F_8 and C_2F_6 ions formed by ionization, is formed near the central electrodes. Therefore the relations between κ and I_t, are thought to be different from those of SF_6 and CO_2.

The dependency of κ on pressure tends to be small as increasing the total corona current. Especially, it is remarkable in the cases of negative polarities, for example, in **Fig. 5** (b). These phenomena can also be explained qualitatively[4] by the space charge effect of the ion cluster near the central electrodes.

As shown in **Fig. 7** (a), at $p=760$ Torr constant, κ at $I_t=$ca. $30\mu A$ is nearly 200, but as the total corona current more than $200\mu A$, κ abruptly decreases to ca. 9. The authors designate it "transition region", as mentioned in the case of N_2⊕ in the previous report.[4] That is, the corona current density increases in the directions of maximum field gradient, $\theta=90°$ and 270° and in the directions of the

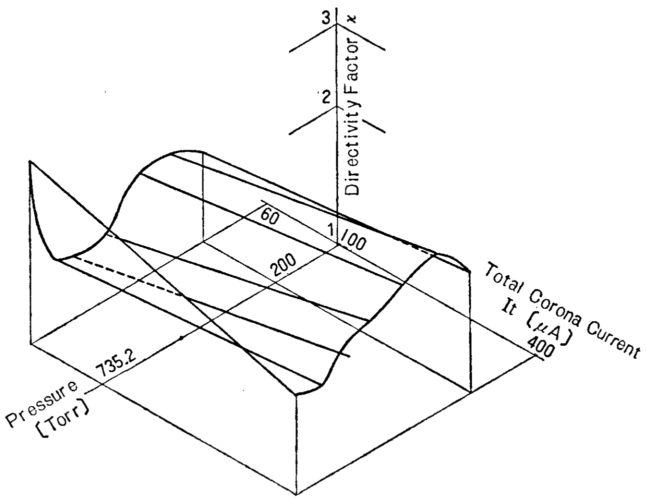

(a) Positive Corona

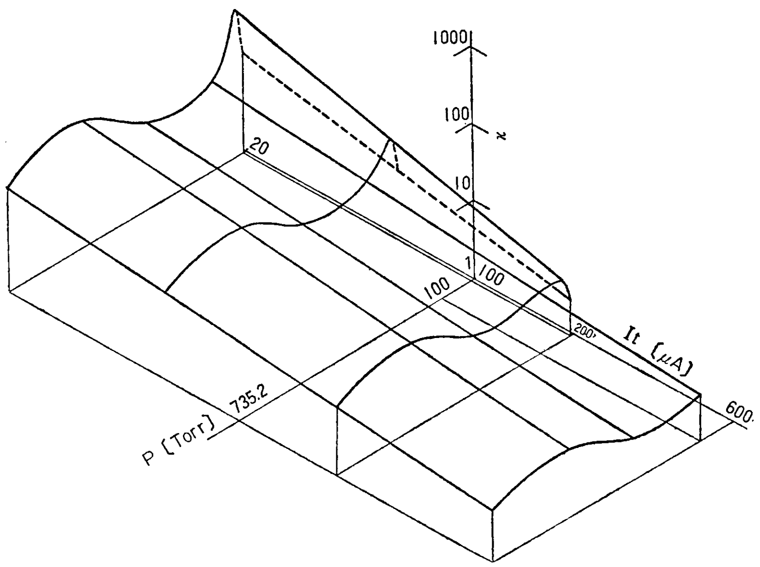

(b) Negative Corona

Fig. 5 Directivity Characteristic in SF_6

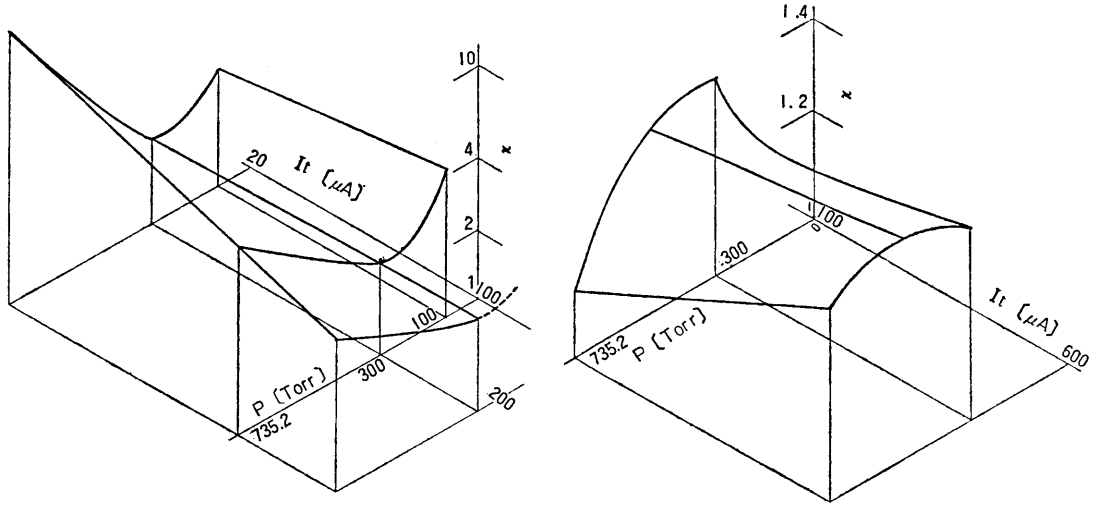

(a) Positive Corona (b) Negative Corona

Fig. 6 Directivity Characteristics in CO_2

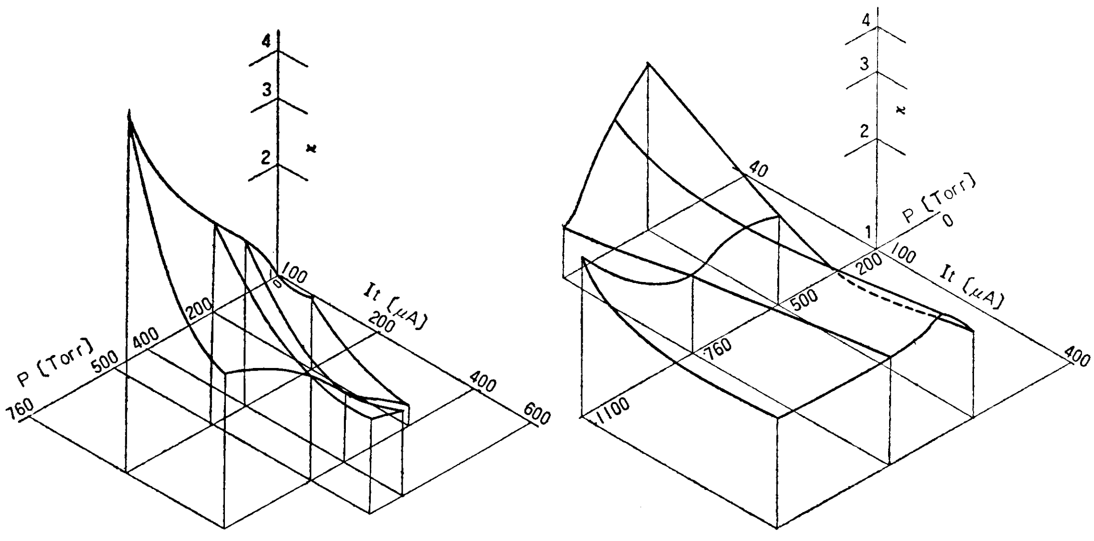

(a) Positive Corona (b) Negative Corona

Fig. 7 Directivity Characteristics in c-C_4F_8

vicinity as increment of I_t. It is only applicable from the corona starting to the transition current, for example, $I_t=300\mu A$ in N_2 and 100 to $200\mu A$ in c-C_4F_8. Therefore from these phenomena in N_2 and c-C_4F_8, the types of corona discharge are thought to have similarities. In order to explain these phenomena, the various informations are needed, for example, wave form of corona current, visual observations of corona discharge and so on.

In **Fig.** 7(a), in overall pressure, κ is seemed to increase as decrement of I_t and the transition region is expected to exist even at lower pressure than 760 Torr. The steady distribution, however, could not be obtained because of the large time-variance of corona current.

The directivity characteristics of C_2F_6 shown in **Fig.** 8 are quite different from those of c-C_4F_8 shown in **Fig.** 7 (a), though both are perfluorocarbon gases. That is, the transition region is not observed in C_2F_6.

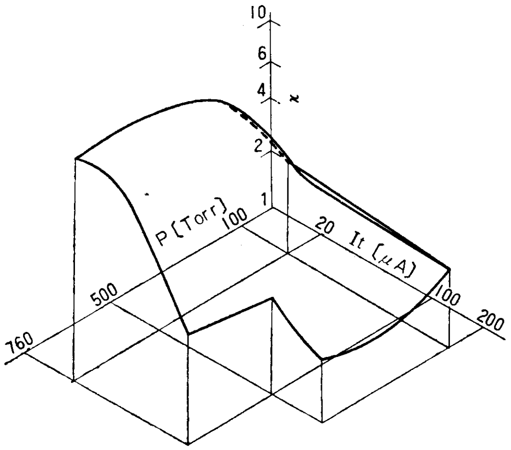

Fig. 8 Directivity Characteristic in C_2F_6

The dependency of κ on pressure in C_2F_6 is the smallest of all gases used and it is noticed that κ decreases abruptly at ca. 100 Torr.

6. Decomposition of c-C_4F_8 Exposed to Corona Discharge

It is described in chapter 2 that c-C_4F_8 is thermal stable and is not toxic in the ordinary state, that is, when little energy is supplied to the gas molecule. On the other hand, when a little energy is supplied to the gas molecule by corona discharge or arc discharge, the gas is probable to be decomposed to some extent.

The authors make an attempt to analyse c-C_4F_8 exposed to corona discharge, because they were confronted with the fact that the gas exposed to corona discharge would produce the decomposed poisonous materials.

Fig. 9 shows an example of the gaschromatographic analysis of c-C_4F_8 exposed to corona discharge. The ordinate axis of the figure is in arbitary scale. This sample gas is collected from c-C_4F_8 in ca. 6 liters exposed to d.c. negative corona discharge with the total corona current $I_t=200\mu A$ for 1 hour, and is put into a conventional gas sampling tube which has been evacuated well. This sample gas is, then, analysed about 18 hours later by means of the gaschromatograph, whose carrier gas is hydrogen.

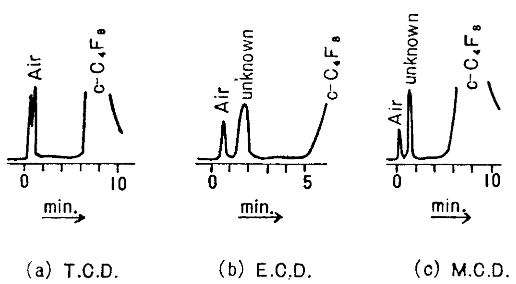

Fig. 9 Gaschromatograms of c-C_4E_8 exposed to Negative Corona Dischage under the condition of $200\mu A\times 1$ hr. and $p=1.5$ kg/cm^2 abs. or ca. 6 liters.

The column condition of the gaschromatograph is 1 meter of length and 4 mm of inner diameter with silica gel (30 to 60 meshes) and 40°C. For the detector are used the Thermal Conductivity Detector (abbrev., T. C. D.), the Electron Capture Detector (E.C.D.) and the Micro Cross-section Detector (M.C.D.), which are in turn connected in series from the column exit.

In **Fig. 9** (a), by the Thermal Conductivity Detector, any unknown materials are not detected, but in **Fig. 9**(b) and (c) an unknown material is detected after the retention time of ca. 2 minutes. It is not yet understood what kind of material this peak shows. The authors, however, can reason about the unknown material that its thermal coductivity is nearly equal to that of hydrogen, and that its boiling point is lower than that of c-C_4F_8 and higher than that of oxygen, as shown in **Fig. 9** (b) and (c).

In pure gas, however, these unknown peaks are not observed.

At present the authors carry on the investigation of the decomposed gas analysis in more detail.

7. Conclusions

(1) The relations between diretivity factor κ, gas pressure p and total corona current I_t in various gases can be clearly expressed by means of the oblique coordinates.

(2) It is pointed out that the characteristics of the directivity factor κ of c-C_4F_8 and C_2F_6 are fairly different from κ of SF_6 and CO_2.

(3) The κ-I_t characteristics of c-C_4F_8 and C_2F_6 can not be always represented by the equation of $\kappa I_t^B=A$.

(4) The κ-I_t characteristics of c-$C_4F_8\oplus$ have the transition region which is similar to the characteristics of $N_2\oplus$.

(5) In both cases of positive and negative

polarities, the corona starting voltages V_s of c-C_4F_8 are always higher than V_s of SF_6 over atomospheric pressure. On the other hand, V_s of C_2F_6⊕ are slightly lower than that of SF_6⊕.

(6) The result of the gaschromatic analysis gives that c-C_4F_8 exposed to corona discharge may contain the decomposed products. The authors will analyse the decomposed products in detail by means of mass spectrometer.

Acknowledgement

The authors wish to thank the Chubu Electric Power Co. for his cooperation in carrying out the gas analysis and the Mitsui-Fluorochemical Co. for supplying c-C_4F_8, C_2F_6 and the informations of perfluorocarbons.

References

(1) S. Muto: Bulletin of Nagoya Instititute of Technology vol. **15** pp.253—258 (1963)

(2) S. Muto: ibid. vol. **16** pp. 264—268 (1964)

(3) S. Muto & T. Tani: ibid. vol. **17** pp. 246—254 (1965)

(4) S. Muto, T. Inaba & T. Shibata: ibid. vol. **19** pp. 283—294 (1967)

(5) H. P. Lemaire & R. L. Livingston: Journal of American Chemical Society. **74** p. 5732 (1952)

(6) Technical Report (B-2) of Mitsui Fluorochemical Co.

(7) J. P. Manion, J. A. Philosophos & M. B. Robinson: IEEE Trans. on Electrical Insulation vol. EI-**2** p.1

(8) J. W. Clayton, Jr., M. A. Delaplame & D. B. Hood: Journal of American Industrial Hyginene Association vol. **21** p. 382 (1960)

(9) Technical Bulletin (EL-1) of Du Pont de Nemours & Company.